PROTEINS: Structure, Function, and Bioinformatics 55:187–197 (2004)

Selection and Affinity Maturation of IgNAR Variable Domains Targeting *Plasmodium falciparum* AMA1

Stewart D. Nuttall,[1,2*] Karen S. Humberstone,[2,3] Usha V. Krishnan,[1,2] Jennifer A. Carmichael,[1,2] Larissa Doughty,[1] Meghan Hattarki,[1] Andrew M. Coley,[2,3] Joanne L. Casey,[2,3] Robin F. Anders,[3,4] Michael Foley,[2,3] Robert A. Irving,[1,2] and Peter J. Hudson[1,2]

[1]*CSIRO Health Sciences and Nutrition, Parkville, Victoria, Australia*
[2]*CRC for Diagnostics, Parkville, Victoria, Australia*
[3]*Department of Biochemistry, La Trobe University, Bundoora, Victoria, Australia*
[4]*CRC for Vaccine Technology, La Trobe University, Bundoora, Victoria, Australia*

ABSTRACT **The new antigen receptor (IgNAR) is an antibody unique to sharks and consists of a disulphide-bonded dimer of two protein chains, each containing a single variable and five constant domains. The individual variable (V_{NAR}) domains bind antigen independently, and are candidates for the smallest antibody-based immune recognition units. We have previously produced a library of V_{NAR} domains with extensive variability in the CDR1 and CDR3 loops displayed on the surface of bacteriophage. Now, to test the efficacy of this library, and further explore the dynamics of V_{NAR} antigen binding we have performed selection experiments against an infectious disease target, the malarial Apical Membrane Antigen-1 (AMA1) from *Plasmodium falciparum*. Two related V_{NAR} clones were selected, characterized by long (16- and 18-residue) CDR3 loops. These recombinant V_{NAR}s could be harvested at yields approaching 5mg/L of monomeric protein from the *E. coli* periplasm, and bound AMA1 with nanomolar affinities ($K_D = \sim 2 \times 10^{-7}$ M). One clone, designated 12Y-2, was affinity-matured by error prone PCR, resulting in several variants with mutations mapping to the CDR1 and CDR3 loops. The best of these variants showed ~10-fold enhanced affinity over 12Y-2 and was *Plasmodium falciparum* strain-specific. Importantly, we demonstrated that this monovalent V_{NAR} co-localized with rabbit anti-AMA1 antisera on the surface of malarial parasites and thus may have utility in diagnostic applications. Proteins 2004;55:187–197.**

Key words: new antigen receptor; bacteriophage display; shark antibody; Apical Membrane Antigen-1; malaria

INTRODUCTION

The New Antigen Receptors (IgNARs) are a unique subset of antibodies found in the serum of nurse and wobbegong sharks.[1–2] In domain structure, these proteins are similar to other immune effector molecules, consisting of homodimers of two polypeptide chains, each comprising a single variable (V_{NAR}) and five constant (C_{NAR}) domains. However, unlike conventional antibodies, there are no associated light chains, and the variable domains do not interact across a V_H–V_L type interface.[3] Thus IgNARs are bivalent and bind target antigen using two separate V_{NAR} domains. Functionally, the closest analogues to IgNARs in mammalian immune repertoires are the camelid V_HH antibodies, which also utilize two separate single variable domains for antigen binding.[4–5] The camelid V_HH antibodies originated from a deletion event removing the first IgG heavy chain constant domain, and as such represent a subset of highly evolved antibody variants.[6] In contrast, the IgNARs are a distinct antibody isotype, evolutionarily distant from other immune molecules and phylogenetically equidistant from T cell receptors and V_L domains. While the V_{NAR} tertiary structure has not yet been determined, it is hypothesized to be similar to antibody V-domains, though the CDR2 loop region appears to have little variability, and there has been extensive mutation of framework residues over a long period of evolutionary time[7] (S. Nuttall, unpublished data).

Because the single V_{NAR} (and camelid V_HH) domains have only half the antigen-binding surface of the mammalian antibody Fv, they compensate by utilizing long CDR3 loops, significantly increased in length compared to mammalian V-domains.[1–2,8–10] These extended loops in both V_{NAR}s and V_HHs are often stabilized by disulphide linkages, either between the CDR1-CDR3 (sharks and camels), or the CDR2-CDR3 (llamas) regions. Additional disul-

Abbreviations: IgNAR, New Antigen Receptor antibody from sharks; V_{NAR}, variable domain of IgNAR antibodies; C_{NAR}, constant domain of IgNAR antibodies; V_HH, variable domain of heavy chain of camelid heavy chain antibodies; V_H, variable domain of heavy chain of conventional antibodies; V_L, variable domain of light chain of conventional antibodies; scFv, recombinant single-chain variable fragment antibody; CDR, complementarity determining region; k_a, association rate constant; *K_a* affinity constant (association); *k_d,* dissociation rate constant; *K_d,* affinity constant (dissociation); ELISA, enzyme-linked immunosorbent assay; FPLC, fast pressure liquid chromatography; PAGE, polyacrylamide gel electrophoresis; AMA1, apical membrane antigen-1 from malarial parasites; Tom70, 70kDa translocase of the outer mitochondrial membrane.

*Correspondence to: Stewart Nuttall, CSIRO Health Sciences and Nutrition, 343 Royal Parade, Parkville, Victoria, Australia. E-mail: Stewart.Nuttall@csiro.au

Received 23 July 2003; Accepted 15 September 2003

phide bonds have also been observed within the extended CDR3 loops (V_{NAR} Type2), and between framework and CDR3 regions (V_{NAR} Type1), and presumably also confer structural stability.[11–12] The combination of small size and extended CDR3 loops produces a highly effective set of immune molecules capable of accessing antigenic sites rarely targeted by conventional antibodies. For example, the camelid repertoire has proven effective at generating antibodies targeting enzyme active sites, as well as a broad range of other antigens.[13] Single V-domains such as mammalian V_H or V_Ls, camelid V_HHs and shark V_{NAR}s are attractive for bioengineering purposes, since they are small (~14–15kDa) half the size of single chain (scFv) fragments derived from V_H–V_L antibodies and capable of production without the potentially labile linker peptide utilized in scFv production.[14–15] Encapsulation of binding affinity into the one domain also means these proteins are robust, for example they readily refold following thermal denaturation, exposure to high pressures, and chemical denaturation.[16] As such, they have been natural candidates for the generation of molecular libraries, using both the established bacteriophage, and emerging ribosome display formats.[14,17] These have had considerable success, particularly using phage display with naive libraries and following immunization of camelids and sharks.[2,18–19]

Previously, we generated large bacteriophage libraries based upon the natural repertoire of V_{NAR} domains from wobbegong sharks.[12] These naïve libraries encapsulated the greatest diversity in the long CDR3 loops and also possessed significant variability within both the framework and CDR1 regions. The CDR3 loops were varied in both length and composition, and were derived from both the natural repertoire and synthetically designed modifications. V_{NAR}s selected from this library specifically bound target antigens with affinities in the mid-to-low nanomolar range.[12,20] Now, to further test the diversity of this library, including investigation of affinity maturation, we sought to pan the library against an important infectious disease target.

The Apical Membrane Antigen-1 (AMA1) from the malarial parasite *Plasmodium falciparum*[21–22] is expressed at the merozoite surface during invasion of erythrocytes, and, while its exact function during invasion is unclear, it is a leading vaccine candidate.[23–25] Polyclonal sera, monoclonal antibodies, and scFv and peptide reagents have all been produced against AMA1, demonstrating that it is immunogenic, and allowing for a thorough comparison between binding reagents. Here, we describe the isolation of two V_{NAR} domains specific for AMA1, and demonstrate that they are antigen-specific, and can be affinity matured to produce a biologically useful targeting protein.

MATERIALS AND METHODS

Equipment and Reagents

Vent and Taq DNA polymerases and all restriction enzymes were purchased from New England Biolabs (Beverley, MA) and used according to the manufacturer's instructions. T4 DNA ligase was from Biotech (Australia). DNA fragment recovery and purification was by QIAquick Gel Extraction Kit, Qiagen (Germany). Small-scale preparations of DNA from *E. coli* were by QIAprep Spin Miniprep Kit, Qiagen (Germany). Purified anti-FLAG antibody was immobilised onto Mini-Leak™ Low resin from Kem-En-Tec (Denmark) following the manufacturer's instructions, to generate anti-FLAG affinity resin. Standard molecular biological techniques were performed as described.[26]

E. coli Strains

The cell line used for library propagation and selection and protein expression was *E. coli* TG1 (K12 *sup*E Δ(*lac-pro*AB) *thi hsd*Δ 5 F′{*tra*D36 *pro*AB$^+$ *lac*I^q *lac*ZΔM15}. *E. coli* transformants were maintained and grown in 2xYT broth supplemented with 100 μg/ml (w/v) ampicillin ±2% (w/v) glucose. Solid media contained 2% (w/v) Bacto-agar. Transformation of *E. coli* was by standard procedures[26] performed using electro-competent cells.

Library Construction and Panning

Construction of the wobbegong V_{NAR} library has been described elsewhere.[20] The total library size was ~4.0×10^8 independent clones. Phagemid particles carrying the V_{NAR}-gene3protein were propagated and isolated by standard procedures.[27] For biopanning of the phagemid library, recombinant *Plasmodium falciparum* AMA1 (3 μg/ml in PBS) was coated onto Maxisorb Immunotubes and incubated at 4°C overnight. Immunotubes were rinsed (PBS), blocked with PBS/2% Blotto (Skim milk powder, Diploma, Australia) for 1 hr at room temperature (RT), and incubated with freshly prepared phagemid particles (in PBS/2% Blotto) for 30 min at RT with gentle agitation followed by 90 min without agitation. After incubation, immunotubes were washed (PBS/0.1% Tween20; 10 washes), followed by an identical set of washes with PBS. Three rounds of panning were performed. Phagemid particles were eluted using 0.1M HCl, pH2.2/1mg/ml BSA, neutralized by the addition of 2M Tris base, and either immediately reinfected into *E. coli* TG1 or stored at 4°C.

Nucleic Acid Isolation and Cloning

Following final selection, phagemid particles were infected into *E. coli* TG1 and propagated as plasmids, followed by DNA extraction. The V_{NAR} cassette was extracted as a *Not*1/*Sfi*1 fragment and subcloned into the similarly restricted cloning/expression vector pGC.[28] DNA clones were sequenced on both strands using a BigDye terminator cycle sequencing kit (Applied Biosystems, USA) and a Perkin Elmer Sequenator. The nucleotide sequences of clones 12Y-1 and 12Y-2 have been deposited in the GenBank database (Accession Numbers AY261681 and AY261682).

Soluble Expression of V_{NAR} Constructs From Expression Vector pGC

Recombinant proteins were expressed in the bacterial periplasm as described.[12,29] Briefly, *E. coli* TG1 starter cultures were grown overnight in 2YT medium/ampicillin (100 μg/mL)/ glucose (2.0% w/v.), diluted 1/100 into fresh

2YT/ 100 μg/mL ampicillin/ glucose (0.1% w/v) and then grown at 37°C/ 200 rpm until OD_{550nm} = 0.2–0.4. Cultures were then induced with IPTG (1mM final), grown for a further 16 hours at 28°C and harvested by centrifugation (Beckman JA-14/6K/10min/4°C). Periplasmic fractions were isolated by the method of Minsky[30] and either used as crude fractions or recombinant protein purified by affinity chromatography using an anti-FLAG antibody-Sepharose column (10 × 1cm). The affinity column was equilibrated in PBS, pH 7.4 and bound protein eluted with ImmunoPure™ gentle elution buffer (Pierce). Eluted proteins were dialyzed against 2 changes of PBS/0.02% sodium azide, concentrated by ultrafiltration over a 3000 Da cutoff membrane (YM3, Diaflo), and analysed by size exclusion chromatography (FPLC) on a pre-calibrated Superdex75 column (Pharmacia) in PBS pH 7.4. Recombinant proteins were analysed by SDS-polyacrylamide gel electrophoresis through 15% Tris/glycine gels.

Enzyme-Linked Immunosorbent Assays

Recombinant *Plasmodium falciparum* AMA1 or negative control protein antigens (0.5–2 μg/well) in PBS were coated onto Maxisorb Immuno-plates (Nunc, Germany) and incubated at 4°C overnight. Plates were rinsed, blocked with PBS/5% Blotto for 1 hr at RT, and incubated with periplasmic fractions or recombinant protein for 1 hr at RT. Plates were rinsed with PBS, washed three times with PBS/0.05% Tween20, and anti-FLAG antibody (1/1000 in PBS/5% Blotto) added. Plates were incubated and washed as above, and the horseradish peroxidase conjugated secondary anti-mouse Fc antibody (Pierce) added (1/1000 in PBS/5% Blotto). Plates were washed again and developed using ABTS (2,2 azino di-(ethyl) benzothiazoline sulphonic acid, Boehringer Mannheim, Germany) or TMB (3,3′,5,5′-tetramethylbenzidine, Sigma) and read at A405/A450 nm.

Biosensor Binding Analysis

A BIAcore™ 1000 biosensor (BIAcore AB, Uppsala Sweden) was used to measure the interaction between V_{NAR} proteins and AMA1. AMA1 at a concentration of 25μg/ml in 10mM sodium acetate buffer, pH 4.5 was immobilized onto a CM5 sensor chip via amine groups using the Amine Coupling Kit (BIAcore AB). The immobilization was performed at 25°C and 5μl/min flow rate. Injection of 20 μl of 25 μg/ml AMA1 coupled 1400RU to the surface. Binding experiments were performed in HBS buffer (10 mM HEPES, 0.15M NaCl, 0.005% surfactant P20, pH 7.4) at 25°C and a constant flow rate of 5 μl/min with a series of analyte concentrations (1346 nM to 84 nM). Regeneration of the AMA1 surface was achieved by running the dissociation reaction to completion before the next injection of analyte. The binding data was evaluated with BIAevaluation 3.0.2.[31]

Error Prone PCR and Library Construction

The 12Y-2 V_{NAR} cassette was mutagenized by error prone PCR using Taq DNA polymerase.[32] Pools of mutated V_{NAR} cassettes were isolated, cut with *Sfi*I/*Not*I, cloned into the phagemid vector pFAB.5c, and transformed into *E. coli* TG1 as previously described.[20] The resulting library (~1.7×10^6 independent clones) showed on average 1–2 residue changes/100 amino acids. Three rounds of panning were performed on immobilized recombinant AMA1 as described above, except that washing stringency was increased over subsequent rounds of panning (20 washes; 22 washes; 24 washes). The selected V_{NAR} cassettes were then rescued, subcloned, and analyzed as above.

Immunofluorescence Assays

Smears of synchronized schizont stage *Plasmodium falciparum* 3D7 parasites were fixed in ice-cold 50% methanol, 50% acetone and probed with ~70pmoles of V_{NAR} 14M-15; or polyclonal rabbit anti-AMA1 serum (1/3000). Slides were incubated for 45 min at RT, and washed five times with 1.5 ml PBS 0.5% BSA (Sigma). For V_{NAR} domains, mouse anti-FLAG (1/1000) was added, incubated as above, and detected using 100 μl of 2 μg/ml anti-mouse alexa fluor 568 (Molecular Probes, Oregon, USA). Rabbit anti-AMA1 was detected using an anti-rabbit FITC conjugate (Sigma, MO, USA). Fluorescence was visualized using a digital camera and fluorescent microscope (Olympus BX50).

Modelling

A search of the pdb database with the 12Y-2 V_{NAR} sequence revealed sequence homologies with T-cell receptors and antibody variable domains, clearly identifying it as an immunoglobulin domain. Template selection for modelling was based on the top-scoring hits by sequence homology and gap length in the CDR regions. The selected pdb file templates represent a mixture of T-cell receptor alpha domains (1B88:B, 1D9K:E, 1H5B:B, 1KB5:A, 1KJ2:A,), Bence–Jones proteins (1BJM:A, 2RHE:), V_H domains (1AY1:H, 1BGX:H, 1IAI:M, 1IGF:J, 1KEN:T, 2IGF:H,) and V_L domains (1F6L:L, 1IFF:L, 1JNL:L, 35C8:L). Representatives of these four classes were included to reduce bias in the modelling, as their representation in the top hits in the pdb search was essentially even and sequence homology was low.

The 12Y-2 models were constructed using the program Modeller [6v2],[33] and included molecular dynamics refinement constrained by the template structures selected over most of the models. The CDR3 region Gly^{92} to Gly^{102} of the 12Y-2 V_{NAR} had no template available and was built entirely *ab initio* by the modeller algorithm using loop models from an internal database. In the immunoglobulins, the CDR H3 loop is variable in length and has to date resisted complete classification predictive of its structure, with prediction of loop conformations mainly confined to the structure of residues proximal to the immunoglobulin framework.[34,35] As the CDR3 loop modelled here did not posses even the basic framework proximal predictive residues used by Morea et al.[34] or Shirai et al.,[35] it was therefore modelled as the lowest energy conformer with no template restraints. Regions representative of the other CDRs and the C'D loop, where alignment gaps were required, had template constraints relaxed and extensive molecular dynamics refinement applied to search for the

lowest energy. For each modelling run five models were generated, and a further five loop models generated for each domain model during refinement. For the 12Y-2 mutant models, the same templates and loop modelling parameters were used as for the wildtype sequence.

RESULTS

Screening V_{NAR} Libraries Against AMA1

To identify novel single-domain binding reagents against immobilized, refolded recombinant *Plasmodium falciparum* AMA1,[22,36] we screened a bacteriophage library displaying IgNAR variable domains (V_{NAR}s). This V_{NAR} library contains $\sim 4 \times 10^8$ independent clones with the major variability encapsulated within the long V_{NAR} CDR3 loop (15–18 residues), with additional contributions from variations within the CDR1 and framework regions.[20] After three rounds of library selection there was a dramatic ($\sim$ four orders of magnitude) increase in the titre of eluted bacteriophages, consistent with positive selection. Thus, V_{NAR} cassettes were excised from the phagemid vector, subcloned into the expression vector pGC, and individual clones sequenced and tested for their ability to bind AMA1.

Of twenty individual clones examined, the majority (55%) were of a single type represented by the clone 12Y-2 [Fig. 1(A)]. The deduced protein sequence revealed a typical V_{NAR} domain of 113 residues, with a large (18 residue) CDR3 loop characterised by the presence of hydrophobic (Tyr, Leu, Phe) residues, and containing the invariant disulphide bridge Cys^{22}–Cys^{82} linking the two β-sheets typical of the immunoglobulin fold. No other cysteine residues were present, which is unlike many V_{NAR} domains, which possess intra-CDR3 or CDR1-CDR3 disulphide linkages. The remaining third round isolates (45%) also encoded one unique V_{NAR} domain, designated 12Y-1, which shared almost identical framework and CDR1 residues with 12Y-2 [Fig. 1(B)]. While the 12Y-1 CDR3 loop is 16 residues in length, two shorter than for 12Y-2, there is at least a superficial resemblance between the CDR3 sequences of the two clones, with a similar mix of hydrophobic amino acids and the absence of cysteine residues [Fig. 1(B)].

Dominant selection of just two clones after only three rounds of biopanning represents an extremely high enrichment factor ($> 10^8$). Such positive selection may be due to high affinity for the target antigen, and/or by a competitive advantage provided by superior expression qualities of the selected proteins. When expressed in *E. coli*, both V_{NAR}s exhibited very high expression levels, above 3–5mg/L of affinity-purified material from the *E. coli* periplasmic space, which was far higher than randomly selected V_{NAR}s from the library. This protein was predominantly in the monomeric state, with no indication of protein aggregation by size exclusion chromatography [Fig. 1(C)]. The 12Y-1 protein expression characteristics and size exclusion chromatography profile were almost identical to those shown for 12Y-2, further emphasising the relatedness of the two proteins (not shown).

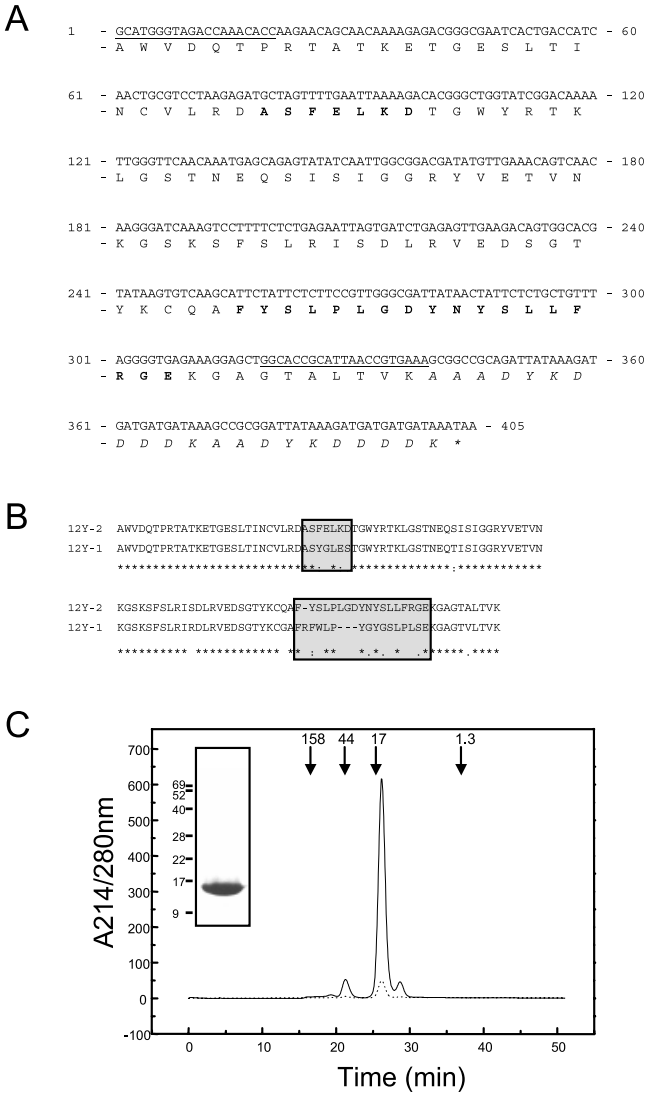

Fig. 1. Nucleotide and deduced amino acid sequences of anti-AMA1 V_{NAR}s. (**A**) Nucleotide and deduced amino acid sequences of the 12Y-2 V_{NAR} variable domain. The conserved termini dictated by the oligonucleotide primer sequences used in library construction are underlined, and the alanine linker and dual octapeptide FLAG tags are italicized. The positions of the CDR-1 and -3 regions are indicated in bold type. (**B**) Alignment of V_{NAR}s 12Y-1 and 12Y-2. Identities (*) and similarities (:) are indicated, and the CDR regions boxed for comparison. (**C**) Size exclusion chromatography of V_{NAR} 12Y-2. Elution profile of affinity-purified 12Y-2 protein on a calibrated Superdex 75 HR10/30 column equilibrated in PBS, pH 7.4 and run at a flow rate of 0.5 ml/min. The peak eluting at 26 min is consistent with a monomeric domain (calculated 12Y-2 M_r of 14,861 Da). The absorbances at A214nm (unbroken line) and A280nm (dashed line) are given in arbitrary units. The inset shows the same sample analyzed by SDS/PAGE through a 15% (w/v) polyacrylamide Tris/glycine gel and stained with Coomassie Brilliant Blue.

V_{NAR}s 12Y-1 and 12Y-2 Specifically Bind AMA1

The specificity of V_{NAR}s 12Y-1 and 12Y-2 was demonstrated by ELISA. Both recombinant proteins reacted specifically with AMA1 but not with several other antigens tested [Fig. 2(A)]. The 12Y-2 response was slightly higher than for 12Y-1, and in addition 12Y-1 exhibited a very slight cross-reactivity to one of the negative control anti-

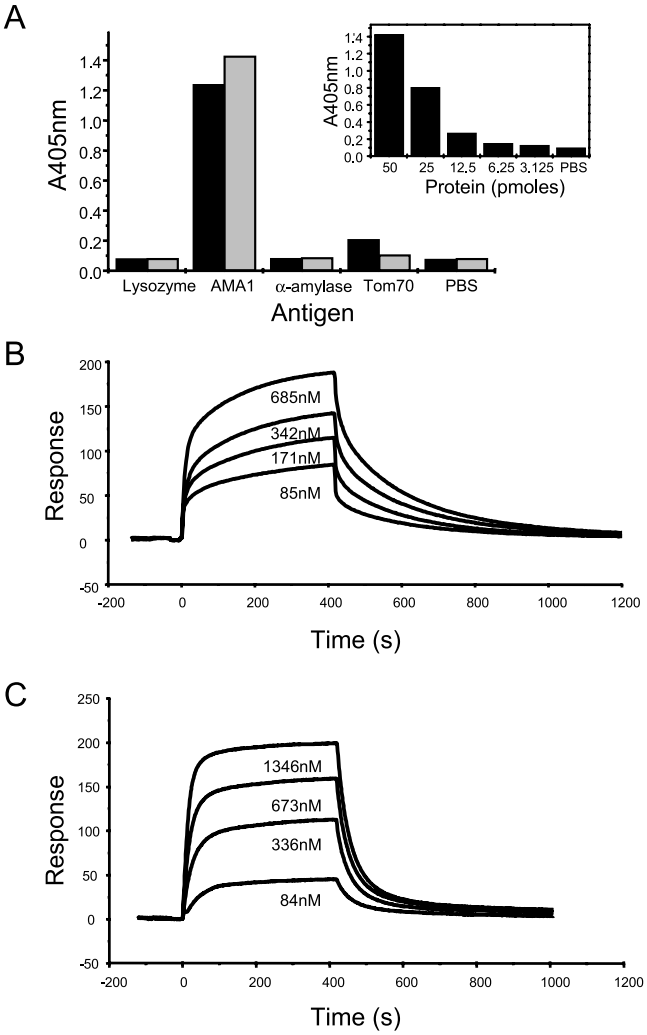

Fig. 2. V_{NAR}s 12Y-1 and 12Y-2 are specific for *P. falciparum* AMA1. (**A**) ELISA comparison of binding of affinity purified proteins 12Y-1 (black) and 12Y-2 (grey) to lysozyme, AMA1, α-amylase, and Tom70. Results represent the average of triplicate wells. The inset shows serial two-fold dilutions of 12Y-2 protein tested for binding to AMA1. Results represent the average of duplicate wells. (**B**) BIAcore sensorgrams showing binding of varying concentrations (685, 342, 171, 85nM) of monomeric V_{NAR} protein 12Y-1 to immobilized AMA1 protein. Binding was measured at a constant flow rate of 5 μl/min with an injection volume of 35 μl. Dissociation was continued with HBS buffer until the response returned to the initial value before injecting the next sample. (**C**) As in (B), except for V_{NAR} protein 12Y-2 at varying concentration (1346, 673, 336, 84nM).

gens [Fig. 2(A)]. The binding kinetics of the 12Y-1/AMA1 and 12Y-2/AMA1 interactions were measured by BIAcore biosensor analysis with the AMA1 protein immobilized by amine coupling to the sensor surface. Analysis of the binding data for varying concentrations of 12Y-1 [Fig. 2(B)] gave a k_a of $2.51 \pm 0.76 \pm 10^4\ M^{-1}s^{-1}$, and a k_d of $4.60 \pm 0.34 \times 10^{-3}\ s^{-1}$ to yield a dissociation constant (K_d) of $2.05 \pm 0.89 \pm 10^{-7}$ M. Similarly, analysis of the binding data for varying concentrations of 12Y-2 [Fig. 2(C)] gave a k_a of $6.32 \pm 1.33 \times 10^4\ M^{-1}s^{-1}$, and a k_d of $1.35 \pm 0.14 \times 10^{-2}\ s^{-1}$ to yield a very similar dissociation constant (K_d) of $2.41 \pm 1.13 \pm 10^{-7}$ M. Thus, the two proteins have very similar expression yields and folding characteristics, and appear to interact with the same epitope on AMA1 (S. Nuttall and K. Humberstone, unpublished data). However, there are differences as 12Y-1 exhibited a very slight cross-reactivity with a non-specific antigen by ELISA [Fig. 2(A)]; and 12Y-2 clone achieves binding through a faster on-rate coupled with a faster off-rate compared to 12Y-1. Since it appears to be easier to improve antibody affinity by selection for a decreased off-rate,[37] we attempted to affinity mature the 12Y-2 binding response.

Affinity Maturation of Clone 12Y-2

For selection of high-affinity variants, a library of mutated 12Y-2 V_{NAR} cassettes was created by error prone PCR. Cloning into phagemid vector pFAB.5c yielded a library size of 1.7×10^6 variants. There were ~1–2 amino acid changes per 100 residues as determined by random clone selection and sequence analysis. After three rounds of panning against immobilized AMA1 under high stringency conditions, there was a 20-fold increase in bacteriophage titre, so individual V_{NAR} cassettes were subcloned and tested for binding by ELISA. From 16 clones tested, several different levels of binding characteristics were observed, ranging from the wild-type level (low binding) to far higher ELISA signals [Fig. 3(A)]. DNA sequencing revealed three types of affinity matured clones (as well as re-isolation of the parental type), represented by clones 14M-5, 14M-8, and 14M-15 [Fig. 3(B)]. All mutations mapped to the CDR1 and CDR3 regions, and no framework mutations were observed. Clone 14M-5 has an Ala27Thr mutation in the CDR1, 14M-8 also has the Ala27Thr mutation in CDR1 and a second mutation Phe100Leu in CDR3. Clone 14M-15 has a single point mutation, Pro90Leu in the CDR3. None of these changes appeared to affect folding of the recombinant proteins, as expression levels (3–5 mg/L) and size exclusion chromatography profiles for the mutants were essentially identical to the parental protein [Fig. 3(C)].

The binding kinetics of the affinity-matured proteins to AMA1 were analyzed by BIAcore. The two CDR3 mutants (14M-8 and 14M-15) both showed approx 10-fold higher affinity for AMA1 than the parent, with dissociation constants (K_d) of 2.86×10^{-8} M and 3.26×10^{-8} M respectively [Fig. 3(D)]. These enhanced affinities were due almost exclusively to slower off-rates. Despite slightly enhanced binding by ELISA [Fig. 3(A), and results not shown], the 14M-5 affinity as measured by BIAcore was essentially identical to the parent 12Y-2 ($K_d = 1.47 \times 10^{-7}$ M), suggesting that on its own the Ala27Thr mutation within the CDR1 has little effect upon affinity. Interestingly, both of the successful affinity-enhancing mutations resulted in the introduction of the motif –YSLLL- into the CDR3 loop. In a further attempt to enhance the 12Y-2 V_{NAR} affinity, a triple mutant incorporating all three mutations was constructed. Surprisingly, while the expression levels and protein stability were again unchanged [Fig. 4(A)], this variant reverted to an affinity for AMA1 almost identical to that of the parental 12Y-2 ($K_d = 1.74 \times 10^{-7}$ M). However, the basis for this interaction appeared to have altered, as this dissociation constant comprised a

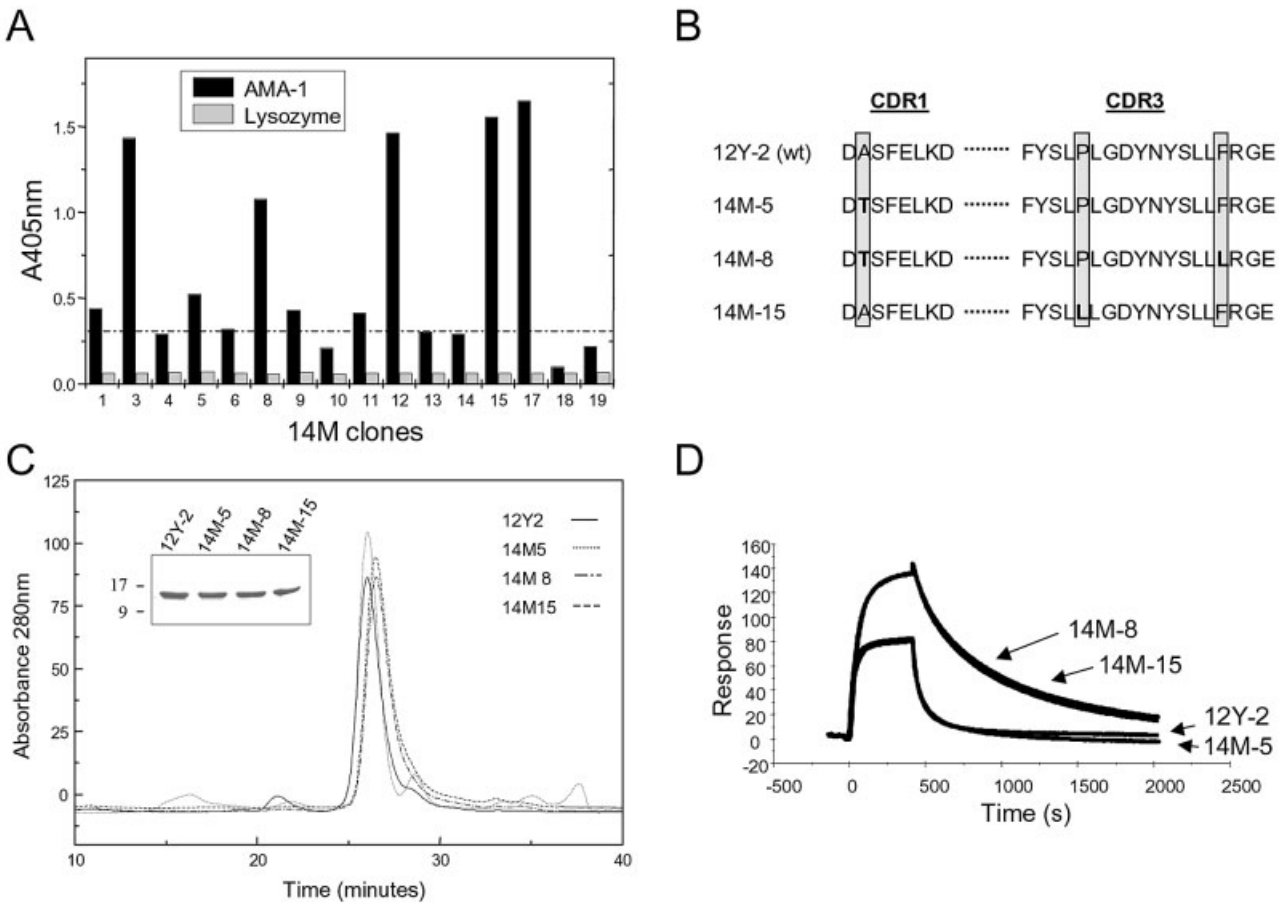

Fig. 3. Affinity maturation of V_{NAR} 12Y-2 by error-prone PCR. (**A**) After three rounds of panning, 16 affinity-matured clones were tested for binding to AMA1 and to lysozyme (negative control antigen). The hatched line represents the parental (12Y-2) response level. (**B**) Deduced amino acid sequences of the CDR-1 and -3 loop regions of the parental (wt) and three mutant proteins (14M-5, 14M-8, and 14M-15). Mutations introduced during the error-prone PCR process are indicated in bold type. (**C**) Size exclusion chromatographs of parental and affinity-matured proteins (see Figure 1 for details). The inset shows the same samples analysed by SDS-PAGE and stained with Coomassie brilliant blue. (**D**) BIAcore sensorgrams comparing the binding of identical concentrations of the parental and mutant proteins to immobilized AMA1 at a constant flow rate of 5 μl/min with an injection volume of 35 μl.

slower association rate in conjunction with a similarly slowed dissociation rate [Fig. 4(B)].

Modelling of 12Y-2 and Variants

To explain more fully the different binding affinities, we modelled the V_{NAR} domain structures of 12Y-2 and variants using molecular dynamics for refinement of the overall model and energy minimisation for loop extensions (Fig. 5). While we recognize that these solutions represent only one possible set of conformations for the long CDR3 loop, we believe that our models clearly show that the different mutations alter the CDR3 loop geometry, leading to an enhanced interaction with the antigen. For example, for clones 14M-8 and 14M-15 the mutations of Phe to Leu and Pro to Leu represent changes to a smaller amino acid and to a less rigid structure respectively. The resultant increased flexibility, while not affecting the on-rate, may have allowed improved presentation of the binding loops to the antigen. We hypothesize that enhanced flexibility allows a better induced fit for the mutated CDR3 and this is supported by data for the triple mutant, where the combination of the two CDR3 mutations may have resulted in poorer presentation of the CDR3 loop to antigen for initial binding (resulting in the slower on rate), which was compensated by the better induced fit leading to the decreased off rate. For the CDR1 loop, the Ala to Thr mutation does not appear to significantly affect the association or dissociation rates, so the slightly larger and polar threonine side chain compared to the wildtype alanine may well have been selected as a neutral mutation. Indeed, in an analysis of over 50 sequences derived from the natural repertoire of Wobbegong sharks, this position 27 is interchangeably occupied by alanine (~26%) or threonine (~55%) in the majority of V_{NAR} proteins (S. Nuttall, unpublished data).

Binding to Native AMA1

The V_{NAR} library and affinity-matured variants were selected against immobilized purified recombinant AMA1. In order to test whether the resulting binding proteins could bind to native AMA1, one of these affinity-matured V_{NAR}s (14M-15) was tested for binding to *Plasmodium*

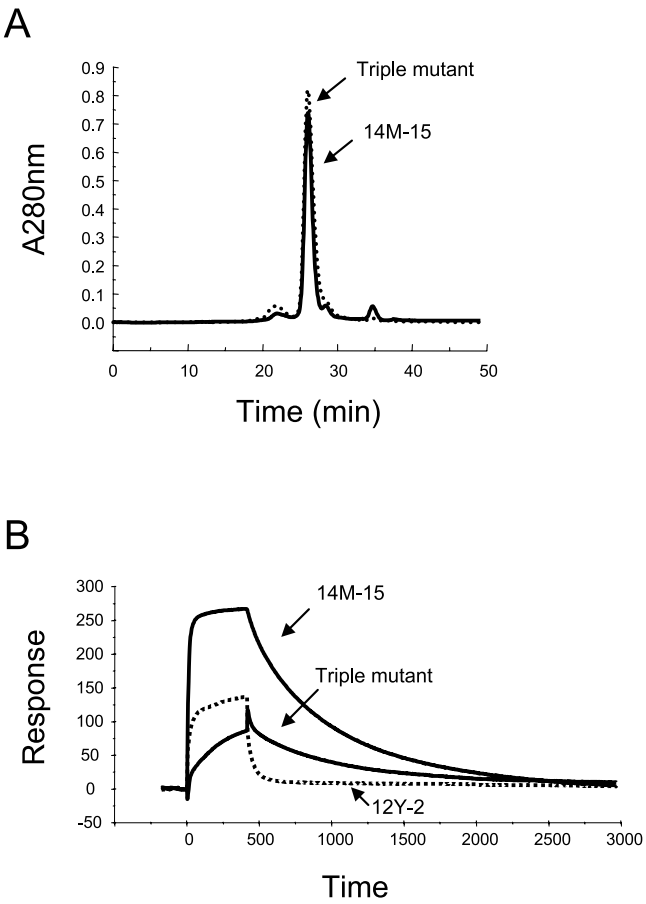

Fig. 4. The 12Y-2 triple-mutant shows parental affinity for AMA1. (**A**) Size exclusion chromatographs of 14M-15 affinity-matured V_{NAR}, and the triple mutant (see Figure 1 for details). (**B**) BIAcore sensorgrams comparing the binding of identical concentrations of the parental (12Y-2), single mutant (14M-15), and triple mutant proteins to immobilized AMA1.

falciparum parasites in an immunofluorescence assay. 14M-15 was incubated with smears of *P. falciparum* parasites that had been cultured *in vitro*, and binding examined by fluorescence. A punctate staining pattern, characteristic of the apical localization of AMA1 at the schizont stage of the parasite life cycle was observed with 14M-15 [Fig. 6(A,B)]. This pattern was indistinguishable from that obtained when rabbit polyclonal antibodies raised against the AMA1 ectodomain were used [Fig. 6(C,D)], and indeed both these signals were found to co-localize [Fig. 6(E,F)]. Thus, 14M-15, while still in its monovalent form, is capable of recognizing the native form of AMA1 in vivo.

Specificity for Different AMA1s

Considerable polymorphisms have been reported in the AMA1 protein across *P. falciparum* strains isolated from the field. These polymorphisms are thought to be due to immune pressure.[38–39] To test whether the V_{NAR}s isolated in this study targeted regions on the AMA1 that are polymorphic or conserved regions V_{NAR} 14M-15 was tested for binding to recombinant AMA1 derived from *P. falciparum* 3D7 (the antigen used in initial selections) and from the *P. falciparum* strains W2MEF, HB3, and D10. Binding was observed to 3D7 and D10 AMA1s, but not protein from the more distantly related strains HB3 and W2MEF (Fig. 7). Surprisingly, a stronger response was observed for D10 AMA1 than for the original antigen. We are unable to account for this higher binding activity, though these two AMA1s are closely related ($>$ 98% identity) and rabbit polyclonal antisera raised against 3D7 AMA1 recognise D10 AMA1 equally strongly[40] (KH & MF, unpublished). Importantly, the lack of binding to reduced and alkylated *P. falciparum* 3D7 AMA1 suggested that V_{NAR} 14M-15 targets a conformational epitope on the AMA1 surface, and indeed when used to probe protein immobilized by western transfer, no AMA1-specific signal was observed.

DISCUSSION

We have selected two low-affinity V_{NAR} domains specific for *P. falciparum* AMA1 from a naïve bacteriophage-displayed library. These V_{NAR}s, 12Y-1 and 12Y-2, closely resemble each other but are significantly different from other V_{NAR}s selected from this library in both their framework and CDR sequences, and from peptides similarly selected by bacteriophage display against AMA1.[22] For example, the 12Y-1 and 12Y-2 CDR3 loop regions are both long (16 and 18 residues respectively) and bear a superficial similarity to each other, most notably in their bias toward bulky hydrophobic amino acid residues and the absence of stabilizing disulphide linkages, either internally or connecting CDR3 to CDR1. More significantly, the two proteins are also almost identical in their non-CDR regions and differ in just two residues (one conservative), despite the forced framework variability encoded in the library design. This indicates a strong selective pressure towards this particular scaffold variant, probably combined with reliance on the particular combination of CDR1/framework regions in maintaining the conformation and orientation of the extended CDR3 loop. Such reliance has also been observed for some camelid V_HH domains, where x-ray crystallographic data shows the CDR3 loop lying across the framework and CDR1 regions.[41] Thus, while our models suggest that the 12Y-2 CDR3 loop can extend stably out into solution, it is at least conceivable that alternatively it folds back across the immunoglobulin fold β-sheet. Recent modelling of the different IgNAR subtype structures suggests that the Type 2 V_{NAR} CDR3s (as here) rely on support from the CDR1 loop, while Type 1 V_{NAR}s show greater interaction between the unusually invariant CDR2 and the CDR3 loops.[7,20] Thus, it will be interesting if the CDR1 variations between V_{NAR}s 12Y-1 and 12Y-2 can be matched to residue and conformational changes in the CDR3 loop. However, the difficulties encountered in attempting to accurately predict the conformational structure of even the modestly sized CDR H3 loops of immunoglobulins,[34,35] suggests that definitive prediction of V_{NAR} CDR3 structures and their interaction with the CDR1 will be problematic. Thus, confirmation of our theories will ultimately depend upon determination of the crystallographic structures of 12Y-1 and 12Y-2 and other V_{NAR} proteins.

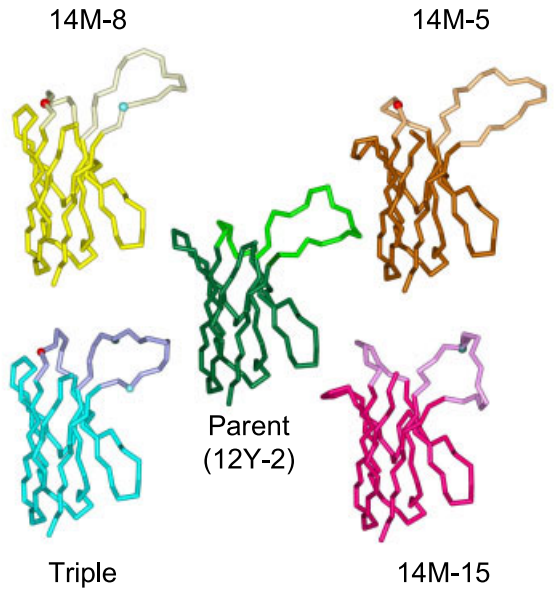

Fig. 5. Models of V_{NAR} domains. V_{NAR} domain 12Y-2 (parental; dark green framework with light green CDRs) and affinity-matured variants were modelled on existing immunoglobulin superfamily variable domain structures. Mutations introduced into the CDR1 (red spheres) and CDR3 (green spheres) are indicated.

Current evolutionary theory indicates that IgNARs are the antibody isotope responsible for the shark adaptive (antigen-driven) immune response, giving rise to high affinity antibodies.[42] Of the other shark antibodies, IgMs (found in monomeric and pentameric forms) are abundant but of low affinity and do not isotype switch, while IgWs (more similar to IgGs in mammals) are present in low amounts in serum.[11] Evidence supporting this pivotal role for IgNARs in the shark immune repertoire includes the rapid somatic hyper-mutation of V_{NAR} domains in response to antigen. This hyper-mutation takes two forms, firstly the generation of extensive CDR3 loop length heterogeneity (compared to embryonic V_{NAR} proteins which have CDR3s of fixed length and limited variability), and secondly, the introduction of single point mutations, in both CDR and framework regions.[11,43] Our naive V_{NAR} library already reflects the CDR3 length heterogeneity component by utilizing V_{NAR} cDNAs from mature sharks, and designed synthetic CDR3s of the most common loop lengths. In this study we also questioned whether we could mimic the natural affinity maturation process by complete variable domain mutagenesis of the low-affinity 12Y-2 V_{NAR} to generate a higher-affinity antibody. Using the well-established and rapid technique of error-prone PCR we identified two distinct mutations in the 12Y-2 CDR3 loop, each resulting in approximately order-of-magnitude

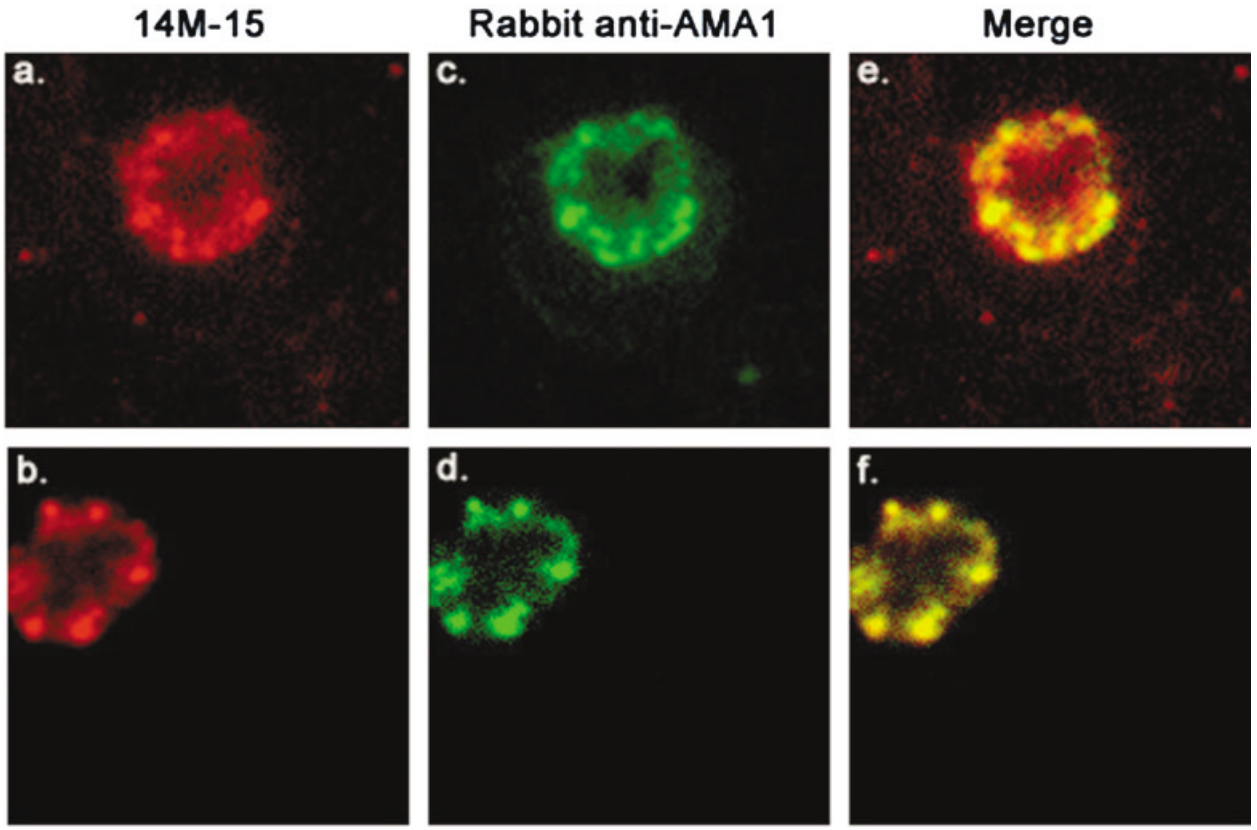

Fig. 6. V_{NAR} 14M-15 targets AMA1 on the surface of *P. falciparum* parasites. Immunofluorescence assays showing V_{NAR} 14M-15 (**A**, **B**) and a polyclonal rabbit anti-AMA1 serum (**C**, **D**) binding schizont-stage *P. falciparum* parasites. Co-localisations of the V_{NAR} and polyclonal serum binding to AMA1 are also shown (**E**, **F**).

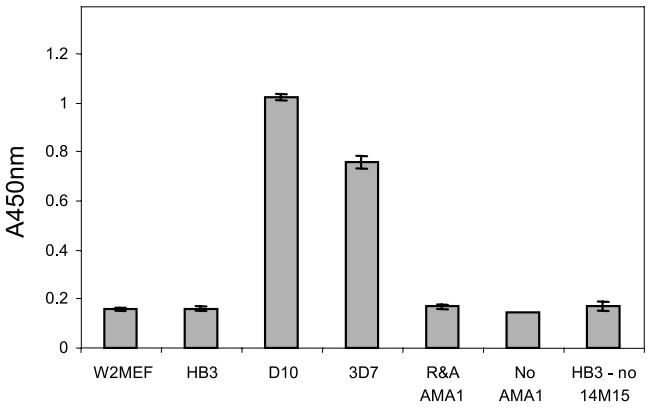

Fig. 7. V_{NAR} 14M-15 targets a variable region of *P. falciparum* AMA1. ELISA comparison of V_{NAR} protein 14M-15 binding to AMA1 derived from *P. falciparum* strains W2MEF, HB3, D10, and 3D7. Binding to reduced and alkylated 3D7 (R&A) is also shown.

enhanced affinities for AMA1. Significantly, no mutations were observed in framework regions, whereas following mutagenesis and re-selection of V_H-V_L antibodies, changes often map to the framework/CDR junctions.[44] To rationalize these results, we suggest that because the extended CDR3 occupies such a significant percentage of the 12Y-2 antigen-binding surface (~16% of total V_{NAR} residues are in CDR3), that CDR3 mutations dominate the available "mutation-space" and overshadow perhaps more subtle variations in stability/expression due to framework mutations. The failure of the 12Y-2 triple mutant to show any further enhanced affinity may then indicate that further CDR3 point mutations with positive affinity gains will be difficult to achieve, and that continued affinity maturation by this technique may then rather yield framework/junction mutations enhancing protein expression levels.[28]

A total of three different 12Y-2 mutations were isolated during our experiments, with the two high-affinity mutations independently introducing the motif –YSLLL- into the CDR3 loop. We are unsure whether this is significant, but certainly both mutations involve increased loop flexibility, and probably act by an enhanced induced fit model, whereby greater loop flexibility allows a tighter interaction with antigen once initial binding has occurred. In this context, it is significant that there is no disulfide linkage between CDR1 and CDR3, or indeed internally within the CDR3, where increased rigidity may be too high a price for the extra stability conferred by introduction of a disulfide bridge. The third mutation generated, an alanine to threonine substitution within the CDR1 loop, was effectively neutral. This particular position within the CDR1 appears to preferably select alanine, threonine, and serine in naturally occurring V_{NAR}s, and again probably represents a residue interacting with the framework, or supporting the antigen-binding loop. In attempts to generate other V_{NAR}s with high affinity toward target antigens, we have also specifically targeted the CDR1 region by window mutagenesis, however, in these cases no mutants with enhanced binding have been observed, and variants were usually compromised in either expression levels or protein solubility.[20] Together, these results strongly support a role for CDR1 in maintaining the CDR3 conformation as much as directly interacting with antigen. We conclude that future affinity maturation should be directed at the entire V_{NAR} domain, without attempts at further site-specific or window mutagenesis. There are a number of strategies available; including error prone PCR as used herein, in vitro mutation by continuous evolution processes, or by natural in vivo systems.[45] Variability introduced in such a manner may stochastically isolate high affinity variants missed by more rational approaches.

The V_{NAR} domains selected against recombinant AMA1 are able to target native AMA1 expressed in schizont stage *P. falciparum* parasites. The ability of the affinity-matured variant to co-localize with a rabbit polyclonal anti-AMA1 antiserum indicates that monovalent V_{NAR}s with mid-nanomolar range affinities are sufficiently specific to act as functional diagnostic reagents. We predict that dimerization of V_{NAR}s through any of a number of well-established recombinant strategies will significantly enhance their functional affinity (avidity), in the manner of bivalent IgGs, while retaining advantages of high stability and small size (~25kDa for V_{NAR} dimers, similar to a monovalent scFv).[15,46–48] The binding reagents that are now available to target *P. falciparum* AMA1 include whole antibodies, Fab and scFv antibody fragments, V_{NAR} domains, and linear peptides.[22,36,49] It will be important to compare the efficacy and affinities of this range of binding molecules, and to elucidate whether they target a single, immunodominant epitope. Certainly, preliminary data from competition studies between the AMA1-specific monoclonal antibodies and peptides suggests the existence of a major immunodominant epitope, and it will be interesting to see whether the V_{NAR}s described here also target this region.

CONCLUSION

This report demonstrates the successful isolation and characterization of two IgNAR antibody variable domains that specifically target the AMA1 antigen from malarial parasites. Our in vitro section from a diverse CDR3-based library, followed by affinity maturation, mirrors the antigen-driven selection/proliferation/maturation process seen in the natural shark immune system. The binding affinities obtained, while only within the mid-nanomolar range, are still biologically useful as evidenced by the in vivo immunofluorescence assays. Moreover, despite the non-additive nature of the affinity-enhancing mutations, we are confident of our ability to further improve the antigen-binding characteristics using sophisticated affinity maturation techniques. Thus, we predict that molecular libraries based on shark antibody V_{NAR} domains will provide stable high-affinity binding reagents for future biotechnological purposes. Natural selection has shaped the IgNAR antibodies to be functional in the high-urea milieu of shark blood[50] suggesting a possible role for these V_{NAR} binding reagents in environmental and biosensors applications, where regeneration of the binding surface is required, in addition to more routine diagnostic applications.

ACKNOWLEDGMENTS

We thank Dr A. Kortt for advice and encouragement, and Mr. N. Bartone for oligonucleotide synthesis.

REFERENCES

1. Greenberg AS, Avila D, Hughes M, Hughes A, McKinney E, Flajnik MF. A new antigen receptor gene family that undergoes rearrangement and extensive somatic diversification in sharks. Nature 1995;374:168–173.
2. Nuttall SD, Krishnan UV, Hattarki M, De Gori R, Irving RA Hudson PJ. Isolation of the new antigen receptor from wobbegong sharks, and use as a scaffold for the display of protein loop libraries. Mol Immunol 2001;38:313–326.
3. Roux KH, Greenberg AS, Greene L, Strelets L, Avila D, McKinney EC, Flajnik MF. Structural analysis of the nurse shark (new) antigen receptor (NAR): molecular convergence of NAR and unusual mammalian immunoglobulins. Proc Natl Acad Sci USA 1998;95:11804–11809.
4. Hamers-Casterman C, Atarhouch T, Muyldermans S, Robinson G, Hamers C, Songa EB, Bendahman N, Hamers R. Naturally occurring antibodies devoid of light chains. Nature 1993;363:446–448.
5. Muyldermans S. Single domain camel antibodies: current status. J Biotechnol 2001;74:277–302.
6. Nguyen VK, Su C, Muyldermans S, van der Loo, W. Heavy-chain antibodies in Camelidae; a case of evolutionary innovation. Immunogenetics 2002;54:39–47.
7. Diaz M, Stanfield RL, Greenberg AS, Flajnik MF. Structural analysis, selection, and ontogeny of the shark new antigen receptor (IgNAR): identification of a new locus preferentially expressed in early development. Immunogenetics 2002;54:501–512.
8. Wu TT, Johnson G, Kabat EA. Length distribution of CDRH3 in antibodies. Proteins 1993;16:1–7.
9. Muyldermans S, Atarhouch T, Saldanha J, Barbosa JA, Hamers R. Sequence and structure of VH domain from naturally occurring camel heavy chain immunoglobulins lacking light chains. Protein Eng 1994;7:1129–1135.
10. Vu KB, Ghahroudi MA, Wyns L, Muyldermans S. Comparison of llama VH sequences from conventional and heavy chain antibodies. Mol Immunol 1997;34:1121–1131.
11. Flajnik MF. The immune system of ectothermic vertebrates. Vet Immunol Immunopathol 1996;54:145–150.
12. Nuttall SD, Krishnan UV, Doughty L, Alley N, Hudson PJ, Pike RN, Kortt AA, Irving RA. A naturally occurring NAR variable domain against the Gingipain K protease from *Porphyromonas gingivalis*. FEBS Lett 2002;516:80–86.
13. Lauwereys M, Arbabi Ghahroudi M, Desmyter A, Kinne J, Holzer W, De Genst E, Wyns L, Muyldermans S. Potent enzyme inhibitors derived from dromedary heavy-chain antibodies. EMBO J 1998;17:3512–3520.
14. Nuttall SD, Irving RA, Hudson PJ. Immunoglobulin VH domains and beyond: design and selection of single-domain binding and targeting reagents. Current Pharmaceut Biotechnol 2000;1:253–263.
15. Hudson PJ, Souriau C. Recombinant antibodies for cancer diagnosis and therapy. Expert Opin Biol Ther 2001;1:845–855.
16. Ewert S, Cambillau C, Conrath K, Plückthun A. Biophysical properties of camelid V(HH) domains compared to those of human V(H)3 domains. Biochemistry 2002;41:3628–3636.
17. Irving RA, Coia G, Roberts A, Nuttall SD, Hudson PJ. Ribosome display and affinity maturation: from antibodies to single V-domains and steps towards cancer therapeutics. J Immunol Methods 2001;248:31–45.
18. Dooley H, Flajnik MF, Porter AJ. Selection and characterization of naturally occurring single-domain (IgNAR) antibody fragments from immunized sharks by phage display. Mol Immunol 2003;40:25–33.
19. Arbabi Ghahroudi M, Desmyter A, Wyns L, Hamers R, Muyldermans S. Selection and identification of single domain antibody fragments from camel heavy-chain antibodies. FEBS Lett 1997;414:521–526.
20. Nuttall SD, Krishnan UV, Doughty L, Pearson K, Ryan MT, Hoogenraad NJ, Hattarki M, Carmichael JA, Irving RA, Hudson PJ. Isolation and characterisation of an IgNAR variable domain specific for the human mitochondrial translocase receptor Tom70. Eur J Biochem 2003;270:3543–3554.
21. Fu Y, Shearing LN, Haynes S, Crewther P, Tilley L, Anders RF, Foley M. Isolation from phage display libraries of scFv antibodies that recognise conformational epitopes in the malaria vaccine candidate, apical membrane antigen-1. J Biol Chem 1997;272:25678–25684.
22. Li F, Dluzewski A, Coley A M, Thomas A, Tilley L, Anders RF, Foley M. Phage-displayed peptides bind to the malarial protein apical membrane antigen-1 and inhibit the merozoite invasion of host erythrocytes. J. Biol Chem 2002;277:50303–50310.
23. Peterson MG, Marshall, VM, Smythe JA, Crewther PE, Lew A, Silva A, Anders RF, Kemp DJ. Integral membrane protein located in the apical complex of Plasmodium fulciparum. Mol Cell Biol 1989;9:3151–3154.
24. Richie TL, Saul A. Progress and challenges for malaria vaccines. Nature 2002;415:694–701.
25. Stowers AW, Kennedy MC, Keegan BP, Saul A, Long CA, Miller LH. Vaccination of monkeys with recombinant Plasmodium falciparum apical membrane antigen 1 confers protection against blood-stage malaria. Infect Immun 2002;70:6961–6967.
26. Ausubel FM, Brent R, Kingston RE, Moore DD, Seidman JG, Smith JA, Struhl K. Current Protocols in Molecular Biology; John Wiley and Sons, NY; 1989.
27. Galanis M, Irving RA, Hudson PJ. Bacteriophage Library construction and selection of recombinant antibodies. current protocols in immunology; John Wiley and Sons, NY; 1997; 17.1.1–17.1.45.
28. Coia G, Ayres A, Lilley GG, Hudson PJ, Irving RA. Use of mutator cells as a means for increasing production levels of a recombinant antibody directed against Hepatitis B. Gene 1997;201:203–209.
29. Nuttall SD, Rousch MJ, Irving RA, Hufton SE, Hoogenboom HR, Hudson PJ. Design and expression of soluble CTLA-4 variable domain as a scaffold for the display of functional polypeptides. Proteins 1999;36:217–227.
30. Minsky A, Summers RG, Knowles JR. Secretion of beta-lactamase into the periplasm of Escherichia coli: evidence for a distinct release step associated with a conformational change. Proc Natl Acad Sci USA 1986;83:4180–4184.
31. Kortt AA, Nice E, Gruen LC. Analysis of the binding of the Fab fragment of monoclonal antibody NC10 to influenza virus N9 neuraminidase from tern and whale using the BIAcore biosensor: effect of immobilization level and flow rate on kinetic analysis. Anal Biochem 1999;273:133–141.
32. Leung DW, Chen E, Goeddel DV. A method for random mutagenesis of a defined DNA segment using a modified polymerase chain reaction. Technique 1989;1:11–15.
33. Šali A, Blundell TL. Comparative protein modelling by satisfaction of spatial restraints. J Mol Biol 1993;234:779–815.
34. Morea V, Tramontano A, Rustici M, Chothia C, Lesk AM. Conformations of the third hypervariable region in the VH domain of immunoglobulins. J Mol Biol 1998; 275:269–294.
35. Shirai H, Kidera A, Nakamura H. Structural classification of CDR-H3 in antibodies. FEBS Lett 1996;399:1–8.
36. Hodder AN, Crewther PE, Anders RF. The specificity of the protective antibody response to apical membrane antigen 1. Infect Immun 2001;69:3286–3294.
37. Hoogenboom HR, de Bruine AP, Hufton SE, Hoet RM, Arends JW, Roovers RC. Antibody phage display technology and its applications. Immunotechnology 1998;4:1–20.
38. Cortes A, Mellombo M, Mueller I, Benet A, Reeder JC, Anders RF. Geographical structure of diversity and differences between symptomatic and asymptomatic infections for *Plasmodium falciparum* vaccine candidate AMA1. Infect Immun 2003;71:1416–1426.
39. Polley SD, Conway DJ. Strong diversifying selection on domains of the *Plasmodium falciparum* apical membrane antigen 1 gene. Genetics 2001;158:1505–1512.
40. Kennedy MC, Wang J, Zhang Y, Miles AP, Chitsaz F, Saul A, Long CA, Miller LH, Stowers AW. In vitro studies with recombinant Plasmodium falciparum apical membrane antigen 1 (AMA1): production and activity of an AMA1 vaccine and generation of a multiallelic response. Infect Immun 2002;70:6948–6960.
41. Desmyter A, Decanniere K, Muyldermans S, Wyns L. Antigen specificity and high affinity binding provided by one single loop of a camel single-domain antibody. J Biol Chem 2001;276:26285–26290.
42. Rumfelt LL, McKinney EC, Taylor E, Flajnik MF. The development of primary and secondary lymphoid tissues in the nurse

shark Ginglymostoma cirratum: B-cell zones precede dendritic cell immigration and T-cell zone formation during ontogeny of the spleen. Scand J Immunol 2002;56:130–148.
43. Diaz M, Velez J, Singh M, Cerny J, Flajnik MF. Mutational pattern of the nurse shark antigen receptor gene (NAR) is similar to that of mammalian Ig genes and to spontaneous mutations in evolution: the translesion synthesis model of somatic hypermutation. Int Immunol 1999;11:825–833.
44. Irving RA, Kortt AA, Hudson PJ. Affinity maturation of recombinant antibodies using E. coli mutator cells. Immunotechnology 1996;2:127–143.
45. Lin H, Cornish VW. Screening and selection methods for large-scale analysis of protein function. Angew Chem Int Ed Engl 2002;41:4402–4425.
46. Kortt AA, Dolezal O, Power BE, Hudson PJ. Dimeric and trimeric antibodies: high avidity scFvs for cancer targeting. Biomol Eng 2001;18:95–108.
47. Arndt KM, Müller KM, Plückthun A. Helix-stabilized Fv (hsFv) antibody fragments: substituting the constant domains of a Fab fragment for a heterodimeric coiled-coil domain. J Mol Biol 2001;312:221–228.
48. Els Conrath K, Lauwereys M, Wyns L, Muyldermans S. Camel single-domain antibodies as modular building units in bispecific and bivalent antibody constructs. J Biol Chem 2001;276:7346–7350.
49. Coley AM, Campanale NV, Casey JL, Hodder AN, Crewther PE, Anders RF, Tilley LM, Foley M. Rapid and precise epitope mapping of monoclonal antibodies against Plasmodium falciparum AMA1 by combined phage display of fragments and random peptides. Protein Eng 2001;14:691–698.
50. Bonaventura J, Bonaventurea C, Sullivan B. Urea tolerance as a molecular adaptation of elasmobranch hemoglobins. Science 1974; 186:57–59.